Spin Transmission Resonance: Theory and Experimental Results in Lithium Metal*

RICHARD B. LEWIS† AND THOMAS R. CARVER
Palmer Physical Laboratory, Princeton University, Princeton, New Jersey
(Received 24 October 1966)

The present status of conduction-electron spin resonance in metals is reviewed. We attempt to show that in terms of practical sensitivity, detection by the transmission method (diffusion of oriented spins into a noise-free region) is superior to the usual reflection technique. Theoretical line shape is derived by a simple phase-adding procedure and from Dyson's theory of nonlocal magnetization, and the latter is made to yield a useful expression for signal power in terms of apparatus parameters. The paper contains a description of the apparatus and a discussion of how it might be improved. A method is given whereby one may experimentally determine values of spin relaxation time and conduction-electron mean free path. The latter determination seems to be more direct than that derived from conductivity measurements, and the beginnings of an interesting study are indicated. Theory and apparatus performance are compared with results obtained in lithium.

I. INTRODUCTION

CONSIDER two microwave cavities with a thin common wall of lithium (Fig. 1). Let their internal fields be such that they have, at the lithium, oscillating magnetic components perpendicular to an external magnetic field $\mathbf{H}_0$. Conduction electrons at the top of the Fermi surface of the lithium have, in the field $\mathbf{H}_0$, a precession (angular) frequency ω_0 given by $\omega_0=\gamma\mathbf{H}_0$, where $\gamma=2\mu/\hbar$ and where μ is the effective electron magnetic moment. Microwaves at the resonance frequency coupled into the first cavity penetrate slightly into the lithium sample and induce in the conduction-electron spins a component of magnetization precessing transverse to the field $\mathbf{H}_0$. In the usual reflection technique one observes radiation from this system emerging from the first cavity (and dispenses with the second). Because the spins are free to diffuse through the sample, however, some of them radiate into the second cavity as well. Observation of this radiation by sensitive equipment is what we call transmission spin resonance. The terms "selective transparency" and "selective transmission resonance" have been used to describe the same effect.

A reflection apparatus requires some device, such as a magic tee or circulator, to separate microwaves incident on the sample cavity from those emerging. These seldom provide more than 60 dB of isolation and are usually microphonic. Thus the system sensitivity is determined by klystron noise and microphonics which far exceed the fundamental limit set by the Nyquist noise of the cavity. In the transmission apparatus, although spin magnetization decays through the sample, it does so generally less rapidly than does the skin-depth electromagnetic field, and the spin signal may be detected in a very quiet cavity. In transmission there are no spurious resonances due to nonmobile surface impurities, and any signal which appears is probably due to mobile spins. Furthermore, symmetric line shapes are more conveniently displayed than in reflection and are often narrower than the intrinsic linewidth, because one observes only *long-lived* spins. Both reflection and transmission methods have common drawbacks in that at low temperatures, in the anomalous skin-depth region, there is considerable mismatch between cavity and sample. The transmission method suffers from the difficulties of sample preparation and microwave leak prevention. In this paper we describe work with lithium as a prototype for studies of conduction resonance in metals generally. The background and present state of these studies follow.

Paramagnetic resonance of the conduction electrons in metals was not observed until 1952,[1] although there were previous attempts to find the effect in the copper walls of a resonance cavity,[2] and in a dispersion of mercury globules.[3] Prior to 1964, only the metals lithium and sodium had been studied systematically, although resonance had been observed in potassium, cesium, and beryllium. Theories of line shape[4] and of conduction spin relaxation[5–7] had been advanced, but only in sodium was there sufficient experimental data to try the theory. Recently there has been renewed interest in conduction-electron resonance in metals, partly because of successful efforts to make much purer samples,[8] and partly because of the virtues of the trans-

* This research was supported by a grant from the National Science Foundation.
† Present address: Department of Physics, Yale University, New Haven, Connecticut.

[1] T. W. Griswold, A. F. Kip, and C. H. Kittel, Phys. Rev. 88, 951 (1952).
[2] E. M. Purcell (private communication relayed by R. H. Dicke).
[3] R. H. Dicke (private communication).
[4] F. J. Dyson, Phys. Rev. 98, 349 (1955).
[5] A. W. Overhauser, Phys. Rev. 89, 689 (1953).
[6] R. J. Elliott, Phys. Rev. 96, 280 (1954).
[7] Y. Yafet, Phys. Rev. 115, 1172 (1959); and in *Solid State Physics: Advances in Research and Applications*, edited by F. Seitz and D. Turnbull (Academic Press Inc., New York, 1963), Vol. 14, p. 1.

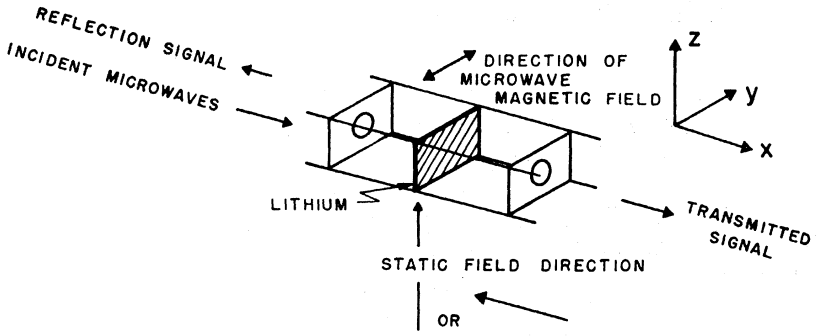

FIG. 1. Schematic arrangement of cavities, magnetic fields, and sample.

mission method of resonance.[9–13] This method was suggested as a possibility by Azbel *et al.*,[9] and independently somewhat later by H. L. Berk and T. R. Carver; it was then experimentally observed by the authors.[11] At present, observation or study of conduction-electron resonance has been made in lithium,[1,11,12,14–24] sodium,[1,14,15,18,19,25,26] potassium,[1,14,15,27] rubidium,[28,29] cesium,[15,28,29] copper,[13] beryllium,[14,30] and aluminum[31] with imminent possibilities for success in magnesium and silver.

II. THEORY

A. Simple Theory

Two questions arise: First, will the resonance be observable at all; and second, how will its shape depend on the physical properties of the sample? Both have simple, approximate answers. Consider the lithium sample shown in cross section in Fig. 2. Suppose that the following approximate, room-temperature parameters apply:

Skin depth	δ	10^{-4} cm
Electron mean free path	Λ	10^{-6} cm
Thickness	θ	10^{-3} cm
Spin relaxation time	U (or T_2)	10^{-8} sec
Fermi velocity	v	10^{8} cm/sec.

It is known that under these conditions it is fairly easy to observe conduction-electron resonance by reflection, and so, as the following argument shows, by transmission also. A spin at the first surface can proceed to the second by random walk, a distance of 10^3 steps. To do this it must make 10^6 steps and so travel a total distance of 1 cm. This will take 10^{-8} sec—just one relaxation time. Thus magnetization at the second surface is comparable to that at the first and a receiver of ordinary sensitivity can detect its radiation, provided that the phases of the spins are preserved as they diffuse across the foil. This *is* the case when the frequency of free precession inside the foil is the same as that of the driving source; all spins have the same phase regardless of history. Now, as the magnetic field is raised above resonance, spins arrive at surface 2 with phases spread and advanced relative to the on resonance condition. The transmitted signal is smaller and phase shifted. By making reasonable assumptions about this phase behavior, we derive the line-shape function for transmission experiments.

Let the time dependence of the microwave field in cavity 1 be $\exp(-i\omega t)$ and the angular frequency of free spin precession be ω_0. Spins at the first surface move in phase with the input field. A spin at the second surface at time t, having diffused across in time Δt, will have phase

$$e^{-i\omega(t-\Delta t)}e^{-i\omega_0\Delta t}=e^{-i\omega t}e^{+i\Delta t(\omega-\omega_0)}. \quad (1)$$

Net magnetization at surface 2 will be the sum over transit times Δt, weighted by the distribution of transit times $n(\Delta t)$, and by the probability that a given spin was not relaxed on its way across, $\exp(-\Delta t/U)$. Assume

[8] W. M. Walsh, Jr., and P. M. Platzman, Phys. Rev. Letters **15**, 784 (1965).
[9] M. Ya Azbel, V. I. Gerasemenkov, and I. M. Lifshitz, Zh. Eksperim. i Teor. Fiz. **32**, 1212 (1957) [English transl.: Soviet Phys.—JETP **5**, 986 (1957)].
[10] M. Ya Azbel and I. M. Lifshitz, in *Progress in Low Temperature Physics* III, edited by C. J. Gorter (Interscience Publishers, Inc., New York, 1961).
[11] R. B. Lewis and T. R. Carver, Phys. Rev. Letters **12**, 693 (1964).
[12] N. S. VanderVen and R. T. Schumacher, Phys. Rev. Letters **12**, 695 (1964).
[13] S. Schultz and C. Latham, Phys. Rev. Letters **15**, 148 (1965).
[14] G. Feher and A. F. Kip, Phys. Rev. **98**, 349 (1955).
[15] R. A. Levy, Phys. Rev. **102**, 31 (1956).
[16] T. R. Carver and C. P. Slichter, Phys. Rev. **92**, 212 (1953).
[17] R. T. Schumacher, T. R. Carver, and C. P. Slichter, Phys. Rev. **95**, 1089 (1954).
[18] R. T. Schumacher and C. P. Slichter, Phys. Rev. **101**, 58 (1956).
[19] T. R. Carver and C. P. Slichter, Phys. Rev. **102**, 975 (1956).
[20] C. Ryter, Phys. Rev. Letters **5**, 10 (1960).
[21] J. L. Hall and R. T. Schumacher, Phys. Rev. **125**, 428 (1962).
[22] R. Hecht, Phys. Rev. **132**, 966 (1963).
[23] R. Hecht and A. G. Redfield, Phys. Rev. **132**, 972 (1963).
[24] R. J. Pressley and H. L. Berk, Phys. Rev. **140**, A1207 (1965).
[25] R. T. Schumacher and W. E. Vehse, Phys. Chem. Solids **24**, 297 (1963).
[26] F. Vescial, N. S. VanderVen, and R. T. Schumacher, Phys. Rev. **134**, A1286 (1964).
[27] R. Dupree and J. E. Cousins, Phys. Letters **14**, 177 (1965).
[28] S. Schultz and M. R. Shanabarger, Phys. Rev. Letters **16**, 178 (1965).
[29] W. M. Walsh, Jr., L. W. Rupp, Jr., and P. H. Schmidt, Phys. Rev. Letters **16**, 181 (1966).
[30] R. Dupree and J. E. Cousins, Phys. Letters **19**, 464 (1965).
[31] S. Schultz (private communication); S. Schultz, G. Dunifer, and C. Latham, Phys. Letters **23**, 192 (1966).

that the electrons obey the diffusion equation,

$$\partial F/\partial t = D\nabla^2 F, \tag{2}$$

where

$$D = \tfrac{1}{3}v\Lambda$$

and consider a spin known to be at $x=0$ at $t=0$. If we ignore the metal surfaces, the probability that it will be found between x and $x+\Delta x$ after a time Δt is

$$\frac{\Delta x}{(\pi D\Delta t)^{1/2}} \exp\left[\frac{-x^2}{4D\Delta t}\right]. \tag{3}$$

We take this to be the probability that the spin has arrived at $x=\theta$. Thus the distribution of arrival times $n(\Delta t)$ is proportional to

$$\frac{1}{(D\Delta t)^{1/2}} \exp\left[\frac{-\theta^2}{4D\Delta t}\right] \tag{4}$$

and complex magnetization at surface 2 is therefore proportional to

$$e^{-i\omega t}\int_0^\infty d(\Delta t)\, \exp[i\Delta t(\omega-\omega_0)]$$

$$\times\left\{\exp\left[-\frac{\theta^2}{4D\Delta t}-\frac{\Delta t}{U}\right]\Big/(\Delta t)^{1/2}\right\}. \tag{5}$$

The integral is the complex sum of Fourier sine and cosine transforms of the expression in curly brackets. From tables[32] the complex magnetization is

$$M \propto C+iS,$$

where

$$C \equiv (1+X^2)^{-1/4}\exp[-\theta f_1/\delta_s]\cos(\theta f_2/\delta_s+\varphi),$$

$$S \equiv (1+X^2)^{-1/4}\exp[-\theta f_1/\delta_s]\sin(\theta f_2/\delta_s+\varphi), \tag{6}$$

$X \equiv U(\omega-\omega_0)$ (a resonance variable scaled to relaxation time),

$$f_1 \equiv \left[\frac{(1+X^2)^{1/2}+1}{2}\right]^{1/2},$$

$$f_2 \equiv \left[\frac{(1+X^2)^{1/2}-1}{2}\right]^{1/2} \mathrm{sgn}X,$$

$\delta_s \equiv (v\Lambda U/3)^{1/2}$ (*spin* depth—the decay length of magnetization),

$$\cos\varphi \equiv (1+X^2)^{-1/4} f_1,$$

and

$$\sin\varphi \equiv (1+X^2)^{-1/4} f_2.$$

[32] H. Bateman, *Tables of Integral Transforms* (McGraw-Hill Book Company, Inc., New York, 1954), Vol. 1, No. 22, p. 16 and No. 32, p. 75.

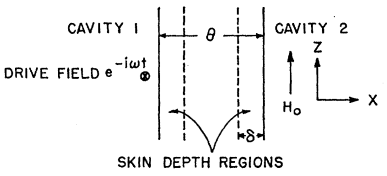

FIG. 2. A section through the sample showing regions traversed by precessing diffusing electrons in different field regions.

The complex amplitude of microwaves radiated by this magnetization is proportional to (6). In a synchronous detection system, this signal beats against a strong reference, $\exp[-i(\omega t+\Phi)]$, where Φ is an arbitrary phase, to give a line shape

$$L = (1+X^2)^{-1/4}\exp[-\theta f_1/\delta_s]\cos(\theta f_2/\delta_s+\varphi+\Phi). \tag{7}$$

The shape is characteristic of transmission spin resonance and independent of assumptions of classical skin-depth propagation, requiring only that the regions containing cavity fields do not overlap or, equivalently, that spins proceed through the sample by diffusion.

B. Extension of the Dyson Results to the Case of Transmission

Dyson[4] has given a general theory of the nonlocal conduction-electron magnetization $\mathbf{M}(\mathbf{r},t)$. He assumed (reasonably for our situation) that magnetization does not affect the penetration of the inducing field, that it is linear in that field, and that spin relaxation can be taken care of by introducing a relaxation time U. He worked out the case of a symmetrically excited flat plate; we modify that result here to the case of a flat plate excited on one side, the geometry appropriate to transmission experiments. The object is to compare line-shape results with those of Sec. II A and to get an explicit expression for the magnitude of second-surface magnetization.

We start with Dyson's equations (54) and (55)[33]:

$$\mathbf{M}(\mathbf{r},t) = \tfrac{1}{2}i\chi\omega_0 \sum_n \psi_n(\mathbf{r})$$

$$\times[\eta_n(\mathbf{s}\cdot\mathbf{h}_n)\mathbf{s}^*-\zeta_n(\mathbf{s}^*\cdot\mathbf{h}_n)\mathbf{s}]e^{-i\omega t}+\text{c.c.}, \tag{8}$$

$\chi \equiv$ volume electronic spin susceptibility, $\omega_0 \equiv \gamma H_0$, spin-resonance angular frequency, $\psi_n \equiv$ the solutions of $\nabla^2\psi_n = -\mu_n\psi_n$ with $\hat{n}\cdot\nabla\psi_n = 0$ at metal surfaces, $\eta_n \equiv [U^{-1}+v\Lambda\mu_n/3-i\alpha]^{-1}$, $\zeta_n \equiv [U^{-1}+v\Lambda\mu_n/3-i\beta]^{-1}$, $\alpha \equiv \omega-\omega_0$, $\beta \equiv \omega+\omega_0$, $\mathbf{s} \equiv \hat{x}-i\hat{y}$.

The $\mathbf{h}_n$ are coefficients of $\mathbf{H}_1$, the microwave field inside the metal, in the space of functions ψ_n; that is $\mathbf{H}_1 = \sum_{n=0}^{\infty}\mathbf{h}_n\psi_n$. For the slab geometry of the sample,

[33] Our symbols ω_0, β correspond to ν, γ of Dyson, and $\mathbf{s}$ is defined for the choice of axes shown in our Fig. 1. It would be superfluous to make here a detailed discussion of either the assumed physical model or the theoretical basis of expression (8). For these, the reader is strongly advised to consult at least the first parts of the excellent Ref. 4.

the functions ψ_n, normalized to unit area, are

$$\Psi_n = a_n \cos(n\pi x/\theta),$$
$$a_0 = (1/\theta)^{1/2},\ a_n = (2/\theta)^{1/2} \quad (n\neq 0), \tag{9}$$
$$\mu_n = (n\pi/\theta)^2.$$

We assume that the exciting field penetrates the metal classically, that is,

$$\mathbf{H}_1 = H_1\hat{y}\exp[-(1-i)x/\delta], \tag{10}$$

where

$$\delta^2 \equiv c^2/2\pi\sigma\omega$$

and, for coefficients $\mathbf{h}_m$, we get

$$\mathbf{h}_m = \int_0^\theta dx\,\psi_m \mathbf{H}_1 \cong a_m \hat{y} H_1 \delta\left[\frac{(1-i)}{2i+(m\pi\delta/\theta)^2}\right], \tag{11}$$

approximating $\int_0^\theta \approx \int_0^\infty$ for $\theta \gg \delta$. Now ignoring the nonresonant term in (8), substituting (11), adopting the convention that physical fields are given by the real parts of complex ones, and evaluating at $x=\theta$:

$$\mathbf{M}(\theta,t) = i\chi\omega_0 \sum_0^\infty \psi_n(\theta)[\eta_n(\mathbf{s}\cdot\mathbf{h}_n)\mathbf{s}^*]$$
$$= \mathbf{s}^*(1-i)(\chi\omega_0 H_1\delta)(\theta/\delta)^2(3\theta^2/v\Lambda)$$
$$\times \sum_{n=0}^\infty a_n(-1)^n \frac{1}{(n^2\pi^2+A)(n^2\pi^2+B)},$$
$$A \equiv 2i(\theta/\delta)^2,$$
$$B \equiv (3\theta^2/v\Lambda U)(1-i\alpha U) = (\theta/\delta_s)^2(1-i\alpha U). \tag{12}$$

The series is summed by breaking each term into partial fractions and summing each group separately by means of the identity[34]

$$\frac{1}{A} + 2\sum_1^\infty \frac{(-1)^n}{n^2\pi^2+A} = \frac{\operatorname{csch}(A)^{1/2}}{(A)^{1/2}}. \tag{13}$$

Inserting numerical values typical of room-temperature lithium, complex second-surface magnetization becomes, in terms of the variables of Sec. II A,

$$M_y = (1-i)(\chi H_1\omega_0 U\delta/\delta_s)(1+X^2)^{-1/4}$$
$$\times \exp[-\theta f_1/\delta_s + i(\theta f_2/\delta_s + \varphi)]. \tag{14}$$

The line shape is identical to that of Eq. (7). The magnitude factor will be needed in the next section.

The physical model and the Dyson formulation apply as long as $\Lambda \ll \theta$, that is, as long as spin transport is by diffusion. The particular approximations leading to (14) require that $(\theta/\delta_s)>1$ and $(\delta_s/\delta)>1$. The first condition is never hard to satisfy; the second will break down in the limit of shorter spin relaxation times or smaller Λ. Where skin-depth fields are anomalous, replacing δ by Λ in (14) will still give some idea of what to expect. It is possible to prepare metals (e.g., magnesium) in which $\Lambda \gg \theta$. In cases of this sort there really is not any diffusion, and surface spin relaxation probably dominates. Our treatment is then of no value and the full machinery of Boltzmann transport theory must be brought to bear on the problem.[9]

The reader should take note of the rather microscopic nature of the derivation of the line shapes, particularly in Sec. II A. Alternative methods[12] employ a Bloch-equation–Maxwell-equations–diffusion-equation point of view on a macroscopic scale,[35,36] and detailed results have recently been published.[37,38] The results of our derivation are in agreement with such results in the regime of the approximations discussed in the previous paragraph. It would seem that the alternative approach is more useful when effects of a finite skin depth must be considered, but it should be borne in mind that the most important results are all contained in the simple and almost physically trivial and obvious Green's-function approach of Sec. II A.[11]

C. Theoretical Signal Power

Magnetization precessing near the second surface of the sample radiates power through cavity 2 to a microwave receiver. We compute this power by a method invented by R. H. Dicke.[39] In what follows, particular application is to the classical skin-depth regime of ESR in metals; however, the main idea will serve in any situation in which a collection of systems interacts with the field supported by a cavity or similar structure.

Consider a cavity matched to a line (Fig. 3) and imagine two distinct sets of fields (denoted by I and II), each consistent with the boundary conditions but corresponding to different driving terms. Maxwell's equations for fields I and II, respectively, when multiplied by $\mathbf{H}$ or $\mathbf{E}$ for fields II and I respectively, yield

$$\mathbf{H}_{II}\cdot(\nabla\times\mathbf{E}_I - i\omega/c\mathbf{H}_I) = \mathbf{H}_{II}\cdot(4\pi i\omega/c)\mathbf{M}_I, \tag{15a}$$
$$\mathbf{E}_{II}\cdot(\nabla\times\mathbf{H}_I + i\omega/c\mathbf{E}_I) = 0, \tag{15b}$$
$$\mathbf{H}_I\cdot(\nabla\times\mathbf{E}_{II} - i\omega/c\mathbf{H}_{II}) = \mathbf{H}_I\cdot(4\pi i\omega/c)\mathbf{M}_{II}, \tag{15c}$$
$$\mathbf{E}_I\cdot(\nabla\times\mathbf{H}_{II} + i\omega/c\mathbf{E}_{II}) = 0, \tag{15d}$$

where the time dependence $\exp(-i\omega t)$ has been divided

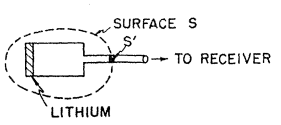

FIG. 3. Cavity and matched line for signal-power computation.

[34] See E. T. Whittaker and G. N. Watson, *A Course of Modern Analysis* (Cambridge University Press, London, 1950), p. 136.

[35] J. I. Kaplan, Phys. Rev. **115**, 575 (1959).
[36] H. C. Torrey, Phys. Rev. **104**, 563 (1956).
[37] M. Lampe and P. M. Platzman, Phys. Rev. **150**, 340 (1966).
[38] G. D. Gaspari, Phys. Rev. **151**, 215 (1966).
[39] R. H. Dicke and R. H. Romer, Rev. Sci. Instr. **26**, 915 (1955).

out. Summing the parts of Eq. (15) according to the scheme $\{(a)-(c)\}+\{(b)-(d)\}$ gives

$$\{\mathbf{H}_{II}\cdot(\nabla\times\mathbf{H}_I)-\mathbf{E}_I\cdot(\nabla\times\mathbf{H}_{II})\}-\{\mathbf{H}_I\cdot(\nabla\times\mathbf{E}_{II})-\mathbf{E}_{II}\cdot(\nabla\times\mathbf{H}_I)\}=(4\pi i\omega/c)(\mathbf{H}_{II}\cdot\mathbf{M}_I-\mathbf{H}_I\cdot\mathbf{M}_{II}). \quad (16)$$

Since, generally, $\nabla\cdot(\mathbf{a}\times\mathbf{b})=\mathbf{b}\cdot(\nabla\times\mathbf{a})-\mathbf{a}\cdot(\nabla\times\mathbf{b})$,

$$\nabla\cdot[(\mathbf{E}_I\times\mathbf{H}_{II})-(\mathbf{E}_{II}\times\mathbf{H}_I)]=(4\pi i\omega/c)(\mathbf{H}_{II}\cdot\mathbf{M}_I-\mathbf{H}_I\cdot\mathbf{M}_{II}). \quad (17)$$

By Gauss's theorem applied over surface S' of Fig. 3

$$\int_{S'}[\mathbf{E}_I\times\mathbf{H}_{II})-(\mathbf{E}_{II}\times\mathbf{H}_I)]\cdot d\mathbf{S}=(4\pi i\omega/c)\int_V(\mathbf{H}_{II}\cdot\mathbf{M}_I-\mathbf{H}_I\cdot\mathbf{M}_{II})dv, \quad (18)$$

the surface integrand being zero except on S', the cross section of the line. So far, this is a general result. Now we specify I and II as follows:

(I) There is no magnetization in the sample and power P_I is incident on the cavity and absorbed.

(II) No power is incident. Magnetization in the cavity radiates power P_{II} which is absorbed by a receiver matched to the line.

Furthermore, let $\mathbf{E}_I=\mathbf{E}_{II}^*$ and $\mathbf{H}_I=\mathbf{H}_{II}^*$. This amounts to the condition, $P_I=P_{II}$, and a special choice of relative phase between the two solutions. Equation (18) now reads

$$2\,\mathrm{Re}\int_{S'}(\mathbf{E}_{II}\times\mathbf{H}_{II}^*)\cdot d\mathbf{S}=-(4\pi i\omega/c)\int_V(\mathbf{H}_I\cdot\mathbf{M}_{II})dv. \quad (19)$$

Since, by Poynting's theorem,

$$P=(c/8\pi)\,\mathrm{Re}\int_{S'}(\mathbf{E}\times\mathbf{H}^*)\cdot d\mathbf{S};$$

$$P_{II}=-(i\omega/4)\int_V(\mathbf{H}_I\cdot\mathbf{M}_{II})dv. \quad (20)$$

Now let H_2 denote the average magnitude of the microwave magnetic field at the surface of the sample in case I. (Subscript 2 indicates that it is cavity 2 we mean.) Stored energy and Q are

$$W=\frac{1}{8\pi}\int_V(E^2+H^2)dv\equiv K_2H_2^2, \quad (21)$$

$$Q_2=\omega W/(\partial W/\partial t)=\omega K_2H_2^2/P_I=\omega K_2H_2^2/P_{II}. \quad (22)$$

Here K_2 is just a geometrical factor. For the case of classical skin depth, the overlap equation (20) becomes, for a sample of area $\mathcal{A}$,

$$P_{II}=-(i\omega/4)\int_{-\infty}^{0}H_2\exp[(1-i)x/\delta]\dot{y}\cdot M_0(\hat{x}+i\dot{y})\mathcal{A}dx=(\omega H_2M_0\mathcal{A}\delta)/4\sqrt{2}\equiv(\omega H_2M_0\mathcal{A}\delta)K_3. \quad (23)$$

We have assumed a uniform magnetization M_0 over the skin-depth region, made a reasonable change in limits of integration, and ignored complex factors modulus 1. The form of (23) is independent of the assumption of classical skin depth, any difficulty being absorbable in $K_3\delta$, a constant times a characteristic overlap distance. Equations (22) and (23) together yield

$$P_{II}\equiv P_{out}=K_3^2\omega(M_0\mathcal{A}\delta)^2Q_2/K_2. \quad (24)$$

This is the power radiated to a receiver by foil magnetization. Factor $(M_0\mathcal{A}\delta)^2$ is the familiar N^2 result for power radiated by N coherent sources; factor Q_2 accounts for radiation from their images in the walls of the cavity.

For purposes of experimental design (24) needs further elaboration. First, with reasonable microwave field levels and spin relaxation times, M_0 is linear in H_1, the average field at the first surface of the sample:

$$M_0=K_4H_1. \quad (25)$$

For the case of classical skin-depth field penetration, Eq. (14) determines K_4. Equations similar to (21) and (22) relate H_1 to power into cavity 1, thus

$$H_1=[P_{in}Q_1/\omega K_1]^{1/2}. \quad (26)$$

Finally, combining (24), (25), and (26), the cavity assembly and sample appear as an attenuator:

$$P_{out}/P_{in}=(K_3^2K_4^2/K_1K_2)Q_1Q_2\mathcal{A}^2\delta^2=\left\{\frac{\chi^2\omega_0^2U^2}{16}\left(\frac{\delta}{\delta_s}\right)^2\right\}\frac{Q_1Q_2\mathcal{A}^2\delta^2}{K_1K_2}\exp[-2\theta/\delta_s]. \quad (27)$$

This is the master equation for the design of transmission experiments on conduction-electron resonance in weakly paramagnetic metals. It may be derived without assuming constant magnetization near surface 2, in the following more elegant way. First expand field $\mathbf{H}_I$ in terms of the set ψ_n of Sec. II B. Then, in Eq. (20) substitute this expansion and the resonant part of the general expression (8) for $\mathbf{M}(\mathbf{r},t)$ (already expanded in the set ψ_n). The x part of the volume integration reduced the resulting double sum to a single one because the ψ_n are orthogonal. The result resembles (12) and can be evaluated in the same way. Reasonable approximations and substitution of (22) and (26) lead again to (27).

Equation (27) indicates how experimental sensitivity depends on sample properties and measurable apparatus parameters. It is interesting to consider what happens to transmitted power as the temperature is lowered.

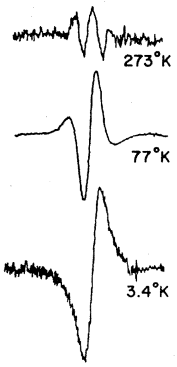

FIG. 4. Qualitative behavior of transmission signals in a relatively thick lithium sample at room temperature, and at liquid-nitrogen and liquid-helium temperatures. The variation of θ/δ_s due to changes in Λ is clear in this sequence. Compare signal to receiver noise for an idea of relative signal size versus temperature. The θ/δ_s ratio is about 12 at room temperature.

Three effects operate: increasing cavity fields due to enhanced Q, decreasing field penetration into the sample, and more efficient transport of spins through it. The first two tend to offset each other since factor $(Q\delta)^2$ remains constant down to that temperature at which the cavity walls attain a limiting value of conductivity. Below this temperature, Q stops improving, while the sample, being usually purer than the cavity walls, continues to exclude more and more of the microwave fields. Thus the quality of the cavity-sample match deteriorates and this factor behaves as $1/\Lambda$. The rest of (27) depends on how U varies with temperature. If spin relaxation time U is determined by impurity scattering and is therefore temperature-independent (as in lithium), there remains the additional factor $(1/\Lambda^2)\exp[-2\theta/(v\Lambda H/3)^{1/2}]$ which may, depending on thickness, either increase or decrease transmitted power as temperature is lowered. We have observed (Fig. 4) that, in fairly thick lithium, transmitted power increases from room-temperature to liquid-nitrogen temperature, then drops sharply at liquid helium. If, on the other hand, spin relaxation is due to phonon scattering and occurs, say, once in every n of these events, then $U=n\Lambda/v$. Approximations leading to (27) require that $(\delta_s/\delta)>1$. In the anomalous case $\delta\rightarrow\Lambda$ and this amounts to the requirement $n\gtrsim\sqrt{3}$. Then we expect the additional factor to be $(1/\Lambda)\exp[-2\sqrt{3}\theta/\Lambda(n)^{1/2}]$. In samples with very short relaxation times (small n), the exponential part dominates and operation at low temperatures increases the chance of observing a resonance.

III. EXPERIMENTAL

A. Apparatus

We describe below our second and more ambitious X-band transmission spectrometer. It is a coherent (or homodyne) device in that its output is sensitive to the phase of the signal emerging from cavity 2. This is done by driving a superheterodyne receiver with power which has been coherently generated from part of the klystron output and which is therefore phase related to the signal to be detected. Figure 5 is a schematic of the equipment with waveguide connections indicated by heavy lines. Construction external to the Dewar is typical except that all waveguide joints carry woven O-rings,[40] and holes at critical points are shrouded with radite,[41] a microwave absorbing material, in order to reduce leakage. High-level parts were leak tested with a horn-fed spectrum analyzer; low-level sections were tested by spraying about 10 mW of main power from a small horn and watching receiver response. A bit of absorbing foam[42] served to cast shadows on suspected areas. We found annoying leakage from tunable crystal holders, slide screw tuners, the back terminations in directional couplers, and some (probably strained) pieces of rubber-covered flexible waveguide. Wrapping these areas with eccosorb has been the usual stopgap.

One waveguide switch shunts a dummy signal into the receiver for sensitivity testing; the other two permit examination and adjustment of the tuning and coupling of either cavity by observing its reflected signal while frequency modulating the klystron. An arrangement of this sort is essential because cooling the cavities or even just evacuating the Dewar is sufficient to shift their resonances. It is very useful to be able to trim and balance the receiver at some particular frequency and then bring both cavities to resonance at this point.

The microwave generator is a Varian V-58 reflex klystron with carefully regulated power supplies. Initially, it was frequency stabilized against an external cavity; we find, however, that the noise performance of the receiver depends on the spectral purity of the microwave source, so now the klystron is phase locked[43] to the output of a Hewlett-Packard 934-A harmonic mixer driven by a 200 Mc/sec stable oscillator.

Signals into the microwave receiver originate in an environment carefully shielded from all other sources of

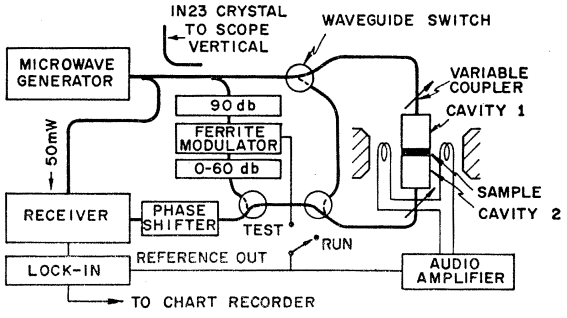

FIG. 5. Simplified schematic diagram of the apparatus. Microwave circuit path shown in heavy lines.

[40] Knitted metal shielding gaskets are made by Technical Wire Products, Inc., 129 Dermody Street, Cranford, New Jersey 07016 and by Metex Electronics, Walnut Avenue, Clark, New Jersey 07066. A conducting plastic gasket we are going to try is made by Emerson and Cuming, 869 Washington Street, Canton, Massachusetts.

[41] Radite, an easy machining ferromagnetic loaded plastic, is made by Radar Design Corporation, 104 Pickard Drive, Syracuse, New York.

[42] Eccosorb, made by Emerson and Cuming.

[43] M. Peter and M. W. P. Strandberg, Proc. IRE 43, 869 (1955).

radiation and free of all but statistical noise. Usually the receiver system output is a line swept over in about 10 sec; therefore, the system bandwidth required is less than 1 cycle per second. Thus at room temperature the noise power in the signal channel is 4×10^{-21} W. Noise power introduced into the signal channel by the receiver limits our experimental sensitivity to 4×10^{-19} W. The receiver (Fig. 6) consists of two balanced mixers, each one a pair of nonlinear devices mounted in the arms of a magic tee. To the left is a sideband generator. Here power from the klystron at 9.3 kmc/sec and from a reference oscillator at 30 Mc/sec are mixed in varactors (Microwave Associates MA 450C) to generate about 5 mW in the upper sideband, 9.3 kMc/sec+30 Mc/sec. If carefully adjusted with a spectrum analyzer, the unwanted fundamental and sideband may be suppressed by at least 40 dB. This balance depends on power level, however, and amplitude fluctuations in either source will upset it. To the right of Fig. 6 is a similar mixer using 1N23E microwave diodes. Here signal power from cavity 2 and the sideband beat together to generate a 30 Mc/sec signal in the diode return circuit. The balanced part of this signal is amplified (up to 130 dB), and detected synchronously with the 30 Mc/sec reference in a balanced bridge. Finally, the bridge output is detected in a lock-in amplifier using as reference the audio sweep frequency of the main field H_0. Notice that everywhere *synchronous* demodulation is used. A signal to be detected never beats with itself but always with some strong, monochromatic phase-related source. This is necessary to preserve the noise bandwidth of the system.[44]

The cavities and sample holder appear in Fig. 7. The cavities are identical and bolt together with the holder between. When assembled, their H fields are perpendicular, so, ideally, there is no electromagnetic coupling even through very thin samples. The 0.400 by 0.900 internal dimensions of the connecting guide taper smoothly to a 3 in. long section of dimensions 0.270 by 0.600. This section, normally beyond cutoff, is nearly filled by a Teflon plunger tapered at its upper end. By varying the unfilled length, unity coupling may be set

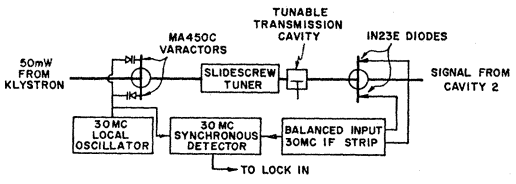

FIG. 6. Detailed schematic diagram of the receiver.

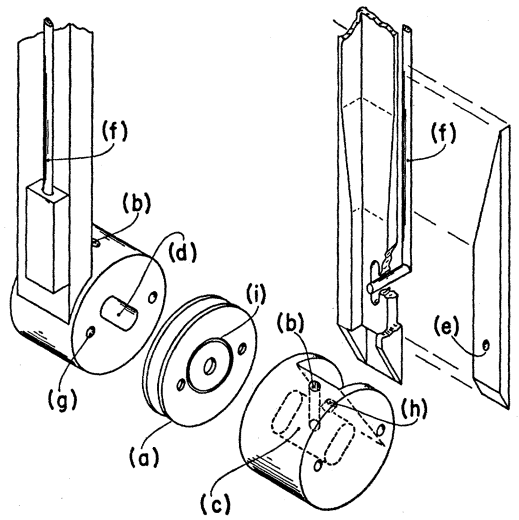

FIG. 7. A schematic assembly diagram of the two cavity and sample structure, showing: (a) sample holder plates, (b) cavity tuning ports for threaded Teflon tuner, (c) and (d) the cavities for excitation and reception, (e) the Teflon coupling inserts, (f) actuating rods for couplers, (g) assembly bolt holes, (h) cavity coupling ports, and (i) ring grooves for indium wire seals.

for any cavity condition.[45] The bottom of the coupling section communicates with the cavity through a $\frac{9}{16}$-in. hole. A $\frac{3}{16}$-in. threaded Teflon rod enters through the broad face of the cavity and tunes it from 9.1 to 9.3 kMc/sec. Both coupling and tuning control rods emerge via $\frac{1}{4}$-in. teflon rods inside 10-in. long brass tubes. These tubes form waveguides well beyond cutoff and entirely prevent microwave leakage. The only demountable joint is that between the cavities and the sample plate (or plates). Rf seals are secured here by cutting O-ring grooves in the sample plates and laying in indium wire[46] of cross section slightly greater than that of the groove. When clamped, the indium flows into a continuous gasket about $\frac{1}{8}$-in. wide and a few thousandths of an inch thick. These joints are microwave tight to at least 170 dB; they are tight to liquid nitrogen, and, we believe, usually tight to helium below the λ point.

This sort of apparatus is worth considering for any microwave spectroscopy of conductors.[47] Our experience may be useful, so we include some suggestions for improvement. First, easy increases in sensitivity lie in increasing input power to the limits of sample heating, electric breakdown of cavity 1, shielding, and cost. Present rf gasketing is, at best, barely adequate. Manufacturers do not usually claim a "shielding effectiveness" of better than 120 dB; although it is hard to know just what this means, the number

[44] This implies that the first detection of the signal should be synchronous, rather than making a second synchronous detection by means, for example, of a lock-in amplifier following an ordinary detector. It is equivalent to the use of a high-frequency lock-in. It is difficult to find a very succinct reference here. See, however, J. L. Lawson and G. E. Uhlenbeck, *Threshold Signals* (McGraw-Hill Book Company, Inc., New York, 1950), MIT Rad. Lab Series, Vol. 24.

[45] J. P. Gordon, Rev. Sci. Instr. **32**, 658 (1961).

[46] We use 0.030-in. wire sold by The Indium Corporation of America, Box 269, Utica, New York.

[47] See, for instance, J. K. Furdyna, Rev. Sci. Instr. **37**, 462 (1966).

suggests that a simple single gasket may not be effective. We recommend enclosing high- and low-level sections in separate, gasketed metal cases and carefully filtering all entering cables. Next, we suggest that each cavity, now assembled of brazed and soft soldered brass, be lost-wax cast as a single piece of beryllium copper and then carefully silver plated. Finally, it is clear that, for transmission work, unless the receiver can read the temperature of cavity 2 down to helium temperature, it is improvable. Ours fails by 40 dB. In planning a modulation system, the designer should realize at the outset what the authors have finally just realized, that the receiver is *not* a radiometer; it is synchronous and its bandwidth is about 10^7 times smaller. Consequently, relative to a radiometer viewing the same temperature source, signal voltages are down by better than 10^{-3}, and both nonstatistical noise (interference) and demodulator noise are much more serious problems. We do not recommend audio modulation of H_0. It cannot be made fast enough to overcome what appears to be $1/f$ noise in the 30-Mc/sec demodulator, and it is too easy to distort a narrow line or never see a wide one. If one tries to amplitude modulate at the input to the receiver there is difficulty with switch noise and with receiver radiation bounced back into the receiver by the switch. This reflected power is troublesome because it is modulated at the switch frequency. Absorptive ferrite isolators will prevent the reflection, but they are expensive and will radiate room-temperature noise into the receiver. If one amplitude-modulates the input to cavity 1, it is hard to prevent modulated reflected power from finding its way back into the sideband generator. In order to avoid this, we suggest that the 30-Mc/sec reference oscillator be used to generate a chain of harmonics and that separate main power and local oscillator klystrons be phase locked to *adjacent* harmonics, thus ensuring both isolation and phase coherence. Alternatively, one might use ac-coupled phase locks with vernier frequencies differing by the frequency of the i.f. strip, in this case 30 Mc/sec. Another scheme worth suggesting attempts to take advantage of the small frequency spread of the signal.

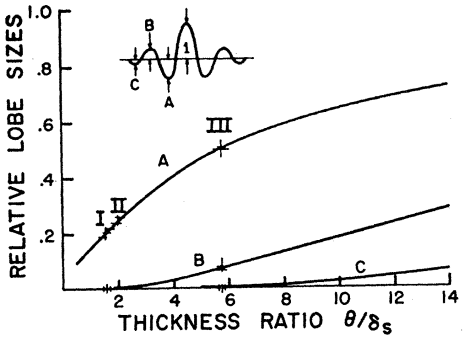

FIG. 8. A plot of the relative lobe sizes at the indicated points of the symmetric derivative lines shape as a function of the thickness ratio θ/δ_s. Marks indicate measured lobe ratios for three samples of lithium.

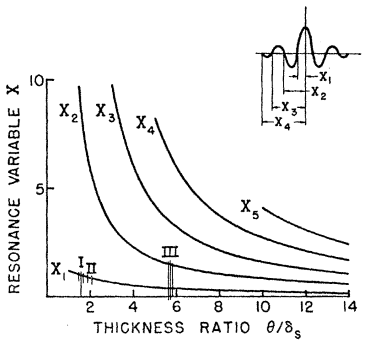

FIG. 9. A plot of the value of the resonance variable X at the zero crossings of the symmetric derivative line shape as a function of the thickness ratio. Marks indicate entering values of the thickness ratio for three samples.

One might manipulate the pump frequency of a very narrow band degenerate parametric amplifier so as to view first the frequency region containing the transmission signal, then another perhaps 100 cps away. Outputs could be compared with a lock-in, and cavity 2 would serve as its own cold load. This sort of "frequency slit modulation" is standard in optical spectroscopy and might also be incorporated in a homodyne receiver by frequency modulating a vernier intermediate frequency oscillator in the phaselock of the local oscillator klystron.

B. Experimental Results with Lithium

We examine now the line shape and transmitted power results. Line-shape data were taken with the field-modulated apparatus described in Sec. III A. At H_0 modulations small relative to line structure, the output of the lock-in is proportional to the derivative of (7) with respect to X, the resonance variable. Thus the line shape L is explicitly given by

$$L=\frac{\exp(-\theta f_1/\delta_s)}{(1+X^2)^{3/2}}$$
$$\times\{[-Xf_1+\tfrac{1}{2}(1+X^2)^{1/2}(\theta X/\delta_s+f_2)]\cos\epsilon$$
$$+[Xf_2-\tfrac{1}{2}(1+X^2)^{1/2}(\theta/\delta_s+f_1)]\sin\epsilon\}, \quad (28)$$

where

$$\epsilon\equiv\theta f_2/\delta_s+\Phi.$$

By manipulating the receiver phase shifter so that $\Phi=\pi/2$ or $\Phi=0$, we get from Eq. (28) recorder traces that are respectively symmetric or antisymmatric about $X=0$. Our line analysis depends on computer studies of the symmetric line, the results of which are displayed in Figs. 8 and 9. To determine the metal parameters, we first measure the relative lobe sizes of the symmetric line, then Fig. 8 determines the ratio θ/δ_s. With this information, Fig. 9 yields the values of X at which zero crossings occur. Since, by Eq. (6), $\Delta X=\gamma U\Delta H_0$, and because an independent proton magnetometer record yields the magnetic field values of the crossings, we compute relaxation times U. Finally, knowing foil thickness and U, and since $\delta_s=(v\Delta U/3)^{1/2}$, we can com-

pute Λ, the electron mean free path. This measurement of Λ is in the absence of applied fields and, given the Fermi velocity v, is independent of any assumption of the number of free electrons per atom. The electrons are tagged by their transverse magnetization and may be thought of as carrying their own clocks, since their precession rate is known. We remark that a similar analysis will certainly work with the output of an amplitude-modulated apparatus. In this case, graphs corresponding to Figs. 8 and 9 must be prepared from Eq. (7). This is probably a better way to proceed for the following reason. As field modulation is increased, a term proportional to the second derivative of the line-shape function appears in the recorder trace. This flattens the central peak and gives incorrect lobe ratios. Such "over-modulation" was avoided here by taking data with successively decreased modulation levels until measured lobe ratios had stabilized. The difficulty is that smaller field modulation means smaller chart recorder deflections, and one is caught between signal-to-noise requirements and those of line-shape distortion.

Room-temperature symmetric traces for three evaporated lithium samples appear in Fig. 10 with derived values of θ/δ_s and U. Dots indicate computer-plotted line shapes generated from the symmetric part of Eq. (28). The right-hand traces are for the same foils made with a 90° change of input phase; the theoretical curves are the antisymmetric part of (28) computed with the same parameters, but, in two cases, adjusted by about 20% in amplitude, a procedure consistent with the gain drifts of the receiver at the time of the run. Line-shape agreement is good and measured values of U are in agreement with previous work.[14] Notice that

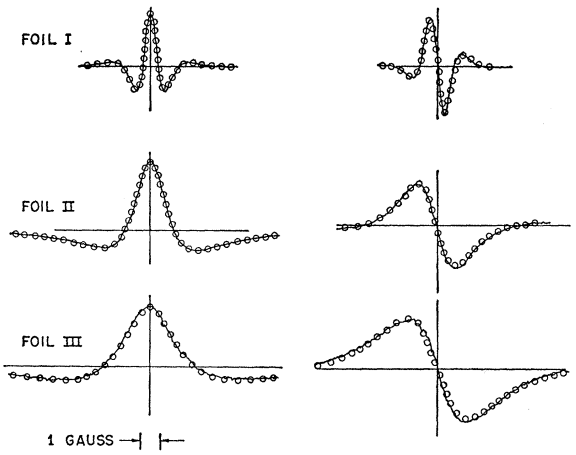

FIG. 10. Measured symmetric and antisymmetric derivative line shapes for three lithium samples. Theoretical curves computed from Eq. (28) are indicated by circles. Foil I: $\theta/\delta_s=5.73\pm0.1$, $U=(5.66\pm0.1)\times10^{-8}$ sec. Foil II: $\theta/\delta_s=2.0\pm0.1$, $U=(3.5\pm0.3)\times10^{-8}$ sec. Foil III: $\theta/\delta_s=1.6\pm0.1$, $U=(2.2\pm0.2)\times10^{-8}$ sec.

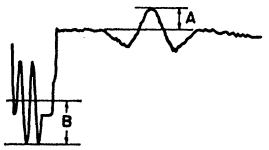

FIG. 11. A direct comparison of power transmitted through a lithium sample with that through a standard attenuator. A indicates 0.8 W transmitted through 91-μ lithium foil at a gain setting of 0.1. B shows 0.8 W attenuated by 120±3 dB at a gain setting of 0.02. Relative amplitude=21, relative power=27 dB, and lithium attenuation measured as 147±3 dB.

relaxation times are determined quite precisely—sufficiently so, at any rate, to disagree with each other. This is not surprising because each sample was distilled from a separate melt.

Values of Λ computed by the preceding method are about one-half that derived from the conductivity of pure lithium.[48] Since these were evaporated samples and since we made no direct measurement of their conductivity, there is little basis for supposing that any interesting discrepancy exists. We plan to repeat this part of the experiment with samples of measured conductivity.

A modest test of predicted absolute attenuation appears in Fig. 11. Amplitude modulation was arranged by moving the ferrite modulator to the receiver input and reducing the effects of reflected receiver radiation by inserting about 90 dB of ferrite isolators. The calibration signal has been disentangled from a zero shift by sweeping the receiver phase shifter through 4π. Measured attenuation is 147±3 dB. Our apparatus uses nearly rectangular brass cavities in the TE_{110} mode at 9.2 kMc. Approximate room-temperature parameters are

$$Q_1=Q_2=2600\pm10\%,$$
$$K_1=K_2=0.11\ \text{cm}^3,$$
$$\mathcal{A}=1.3\ \text{cm}^2.$$

The lithium sample was rolled from undistilled, 99% pure metal. It had the following properties:

$\theta=8.1\times10^{-3}$ cm	(measured)
$\delta=1.5\times10^{-4}$ cm	(computed)
$U=2\ \times10^{-8}$ sec	(typical)
$\Lambda=1.1\times10^{-6}$ cm	(Ref. 48)
$\chi=2.1\times10^{-6}$ esu	(Ref. 18)
$\sigma=1.1\times10^{17}$ sec^{-1}	(in esu, Ref. 48)

Transmitted power computed from (27) is -138 ± 8 dB, where the uncertainty is assigned on the basis of a 10% uncertainty in δ_s.

[48] C. Kittel, *Introduction to Solid State Physics* (John Wiley & Sons, Inc., New York, 1956), p. 240.